Electronic Supplementary Material (ESI) for ChemComm.

Hydrogen Production from Water using a Bis(imino)pyridine Molybdenum Electrocatalyst

Electronic Supplementary Information

Raja Pal, Joseph A. Laureanti, Thomas L. Groy, Anne K. Jones, Ryan J. Trovitch**

School of Molecular Sciences, Arizona State University, Tempe, Arizona 85287

anne.katherine.jones@asu.edu, ryan.trovitch@asu.edu

EXPERIMENTAL SECTION

General Considerations. All chemical manipulations were performed in an MBraun glovebox under an atmosphere of purified nitrogen. Diethyl ether, pentane, tetrahydrofuran, and toluene (Sigma-Aldrich) were dried using a Pure Process Technology (PPT) solvent system, and stored in the glove box over activated 4Å molecular sieves and metallic sodium (Alfa Aesar) before use. Acetonitrile was dried by distillation over calcium hydride. Acetonitrile-d_3, benzene-d_6 (Cambridge Isotope Laboratories) were dried over 3Å and 4Å molecular sieves, respectively, and metallic potassium (for benzene-d_6, Sigma-Aldrich) prior to use. The compounds 2,6-diacetylpyridine (TCI America), Celite (Acros Organics), silver hexafluorophosphate (Strem), and tetrabutylammonium hexafluorophosphate ($TBAPF_6$) (Sigma-Aldrich) were used without further manipulation and 3-(diphenylphosphino)-1-propanamine,[1] ^{Ph2PPr}PDI[2] and [(^{Ph2PPr}PDI)MoI]I (**1**)[3] were prepared according to literature procedures. Solution phase ^{1}H, ^{13}C, and ^{31}P nuclear magnetic resonance (NMR) spectra were recorded at room temperature on either a 400 MHz or 500 MHz Varian NMR Spectrometer. All ^{1}H and ^{13}C NMR chemical shifts are reported relative to $Si(CH_3)_4$ using ^{1}H (residual) and ^{13}C chemical shifts of the solvent as secondary standards. ^{31}P NMR data are reported relative to H_3PO_4. Elemental analyses were performed at Robertson Microlit Laboratories Inc. (Ledgewood, NJ).

Electrochemistry. Electrochemical investigations were carried out under a nitrogen or hydrogen atmosphere using a PG-STAT 128N Autolab electrochemical analyzer. A conventional three-electrode cell was used for recording cyclic voltammograms. Glassy carbon working electrodes (3 mm diameter) were prepared by successive polishing with 1.0 and 0.3 μm alumina slurries (Buehler), followed by sonication (5 min) in ultrapure water after each polishing step. The supporting electrolyte was 0.1 M $TBAPF_6$ in acetonitrile. The Ag/Ag^+ pseudoreference electrode was prepared by immersing a silver wire anodized with AgCl in a glass sheath equipped with a Vycor or CoralPor frit (BASi: West Lafayette, IN) and loaded with 0.1 M $TBAPF_6$ in acetonitrile. A platinum wire was used as the counter electrode. All potentials are reported relative to the ferrocene/ferrocenium ($Fc^{+/0}$) couple as a reference.

Controlled potential experiments were completed in a custom-made, airtight electrochemical cell equipped with a gas-tight sampling port. The electrochemical cell mirrors the conventional three-electrode cell described above. The quantity of H_2 produced was determined by sampling the

headspace *via* gastight syringe at the end of the experiment. Headspace gas was analyzed with an SRI model 310 gas chromatograph (GC) equipped with a thermal conductivity detector (TCD) and a 6' molecular sieve 13X packed column; argon was used as the carrier gas. The GC-TCD was calibrated using known concentrations of H_2 in N_2.

Open circuit potential determination. Open circuit potentials (OCP) were determined using the method described by Roberts and Bullock in a 10 mL four-neck, airtight electrochemical cell equipped with three electrodes as described above and a gas-tight sampling port.[4] An acetonitrile solution containing 0.1 M $TBAPF_6$ was purged with 1 atm H_2 gas. The working electrode was then connected to the platinum counter electrode (now the working electrode) and water was introduced to the desired molar concentration. The OCP was recorded following stabilization. Potentials were adjusted to the $Fc^{+/0}$ reference scale using a cyclic voltammogram of Fc at each water concentration obtained with glassy carbon as the working electrode. Results are provided in Table S4.

X-ray crystallography. Single crystals suitable for X-ray diffraction were coated with polyisobutylene oil in the glovebox and transferred to glass fiber with Apiezon N grease before mounting on the goniometer head of a Bruker APEX Diffractometer (Arizona State University) equipped with Mo Kα radiation. A hemisphere routine was used for data collection and determination of the lattice constants. The space group was identified and the data was processed using the Bruker SAINT+ program and corrected for absorption using SADABS. The structures were solved using direct methods (SHELXS) completed by subsequent Fourier synthesis and refined by full-matrix, least-squares procedures on [F^2] (SHELXL). The solid state structure of **2** was found to feature two acetone molecules, one of which was modelled over three partially occupied sites (two were refined anisotropically with H atoms). Parameters for **2** (CCDC-1480114) and **3** (CCDC-1480115) are provided in Table S1.

Preparation of [(^{Ph2PPr}PDI)MoO][PF_6]$_2$ (2). A 20 mL reaction vial was wrapped with electrical tape, and charged with 0.090 g (0.093 mmol) of **1**, 0.012 g (0.1 mmol) of styrene oxide, and 3 mL of acetonitrile. To this solution, 0.048 g (0.19 mmol) of $AgPF_6$ in 5 mL of acetonitrile was added slowly while stirring. The reaction vial was sealed and allowed to heat at 60 °C for 12 h. The orange solution was cooled to room temperature for precipitation of AgI, after which the solution was filtered through Celite and dried under vacuum. A bright orange compound was

extracted from acetone and dried under vacuum to afford 0.069 g (73%) of solid identified as **2**. Single crystals suitable for X-ray diffraction were grown from acetone/THF at -15 °C. Elemental analysis for $C_{39}H_{41}N_3MoP_4OF_{12}$: Calcd. C, 46.12%; H, 4.07%; N, 4.14%. Found: C, 46.40%; H, 4.16%; N, 4.05%. ^{1}H NMR (acetonitrile-d_3, 400 MHz): 7.82 (m, 4H, *Ph*), 7.60 (m, 9H, *Ph*), 7.44 (t, 7.6 Hz, 2H, *Ph*), 7.30 (t, 7.6 Hz, 4H, *Ph*), 7.21 (t, 8.0 Hz, 1H, *Py*), 6.30 (d, 8.0 Hz, 2H, *Py*), 4.25 (d, 13.2 Hz, 2H, CH_2), 3.65 (m, 2H, CH_2), 3.44 (m, 2H, CH_2), 2.59 (m, 4H, CH_2), 2.35 (m, 2H, CH_2), 2.10 (s, 6H, CH_3). ^{13}C NMR (acetonitrile-d_3, 100.49 MHz): 172.4 (*C*=N), 155.2 (*Ar*), 145.2 (*Ar*), 134.3 (t, 6.7 Hz, *Ph*), 133.3 (*Ar*), 133.2 (t, 2.5 Hz, *Ph*), 132.8 (*Ar*), 131.9 (t, 20.9, *Ph*), 130.8 (t, 5.0 Hz, *Ph*), 130.7 (t, 5.0 Hz, *Ph*), 126.7 (t, 23.1 Hz, *Ph*), 126.2 (*Ar*), 57.3 (NCH_2), 29.0 (t, 10.6 Hz, PCH_2), 26.8 (PCH_2CH_2), 16.6 (*C*H_3). ^{31}P NMR (benzene-d_6, 161.78 MHz): 22.9 ppm (s, *P*Ph_2), -143.6 (sept, J_{PF} = 705 Hz, *P*F_6).

Preparation of (^{Ph2PPr}PDI)MoO (3). *Method 1.* A 20 mL vial was charged with 0.0038 g (0.098 mmol) of freshly cut potassium, 0.0122 g (0.095 mmol) of naphthalene, and 2 mL of THF. The solution was stirred for 30 min to form green potassium naphthalenide solution. To it, 0.051 g (0.050 mmol) of **2** in 10 mL of THF was slowly added and the mixture was stirred at 25 °C for 24 h. The resulting brown solution was filtered through Celite and the solvent was removed *in vacuo*. After washing with cold pentane and drying, 0.025 g (68%) of a brownish-red solid identified as **3** was isolated. *Method 2*. A 20 mL vial was charged with 0.030 g (0.042 mmol) of (κ^6-*P*,*N*,*N*,*N*,*C*,*P*-^{Ph2PPr}PDI)MoH,[3] and dissolved in 2 mL of toluene. Following addition of 0.001 mL H_2O, the mixture was stirred at ambient temperature for 12 h. The reddish-brown solution was filtered through Celite, and dried *in vacuo*. After washing with cold pentane, 0.025 g (81%) of a brown solid identified as **3** was isolated. Single crystals suitable for X-ray diffraction were grown from a concentrated ether solution at -35 °C. Elemental analysis for $C_{39}H_{41}N_3MoP_2O$: Calcd. C, 64.55%; H, 5.69%; N, 5.79%. Found: C, 63.54%; H, 5.60%; N, 5.30%. ^{1}H NMR (benzene-d_6, 500 MHz): 7.88 (m, 4H, *Ph*), 7.66 (d, 8.0 Hz, 2H, *Py*), 7.39 (br, 1H, *Py*), 7.07 (t, 7.5 Hz, 4H, *Ph*), 7.01 (m, 2H, *Ph*), 6.67 (t, 7.5 Hz, 2H, *Ph*), 6.53 (d, 7.5 Hz, 4H, *Ph*), 5.58 (t, 12.5 Hz, 2H, NCH_2), 5.45 (m, 4H, *Ph*), 4.85 (d, 12.5 Hz, 2H, NCH_2), 3.35 (t, 12.0 Hz, 2H, CH_2), 2.80 (s, 6H, CH_3), 2.20 (br, 2H, CH_2), 1.79 (br, 2H, CH_2), 1.59 (m, 2H, CH_2). ^{13}C NMR (benzene-d_6, 100.49 MHz): 138.95 (t, 10.0 Hz, *Ph*), 136.64 (*Ar*), 133.07 (t, 7.0 Hz, *Ar*), 132.41 (t, 7.0 Hz, *Ph*), 130.01 (*Ar*), 129.26 (*Ar*), 128.84 (*Ar*), 128.64 (m, *Ph*), 128.3 (*Ar*), 128.18 (*Ar*), 127.58 (t, 3.0 Hz, *Ph*), 112.60 (*Py*), 109.07 (*Py*), 58.53 (NCH_2), 28.69 (t, 8.0 Hz,

P*C*H_2), 27.41 (PCH_2*C*H_2), 13.50 (*C*H_3). ^{31}P NMR (benzene-d_6, 161.78 MHz): 4.88 ppm (s, *P*Ph_2).

X-RAY CRYSTALLOGRAPHIC DATA

Table S1. Crystallographic Data for [(^{Ph2PPr}PDI)MoO][PF_6]$_2$ (**2**) and (^{Ph2PPr}PDI)MoO (**3**).

	2	**3**
chemical formula	$C_{45}H_{51.47}F_{12}MoN_3O_3P_4$	$C_{39}H_{41}MoN_3OP_2$
formula weight	1130.18	725.63
crystal dimensions	0.224 x 0.177 x 0.113	0.20 x 0.13 x 0.05
crystal system	monoclinic	monoclinic
space group	P 1 21/c 1	P 1 21/c 1
a (Å)	15.3031(6)	11.1519(11)
b (Å)	15.9629(6)	16.9788(14)
c (Å)	20.6295(8)	18.2450(13)
α (deg)	90	90
β (deg)	104.6220(10)	105.844(5)
γ (deg)	90	90
V (Å^3)	4876.2(3)	3323.4(5)
Z	4	4
T (°C)	123.(2)	100.(2)
ρcalcd (g cm^{-3})	1.539	1.450
μ (mm^{-1})	0.489	0.528
reflections collected	38574	21534
data/restraints/parameters	8623/1/600	5888/0/417
R_1 [I > 2σ(I)]	0.0448	0.0520
wR_2 (all data)	0.1233	0.1110
Goodness-of-fit	1.066	0.975
Largest peak, hole (eÅ^{-3})	1.630, -0.644	0.559, -0.586

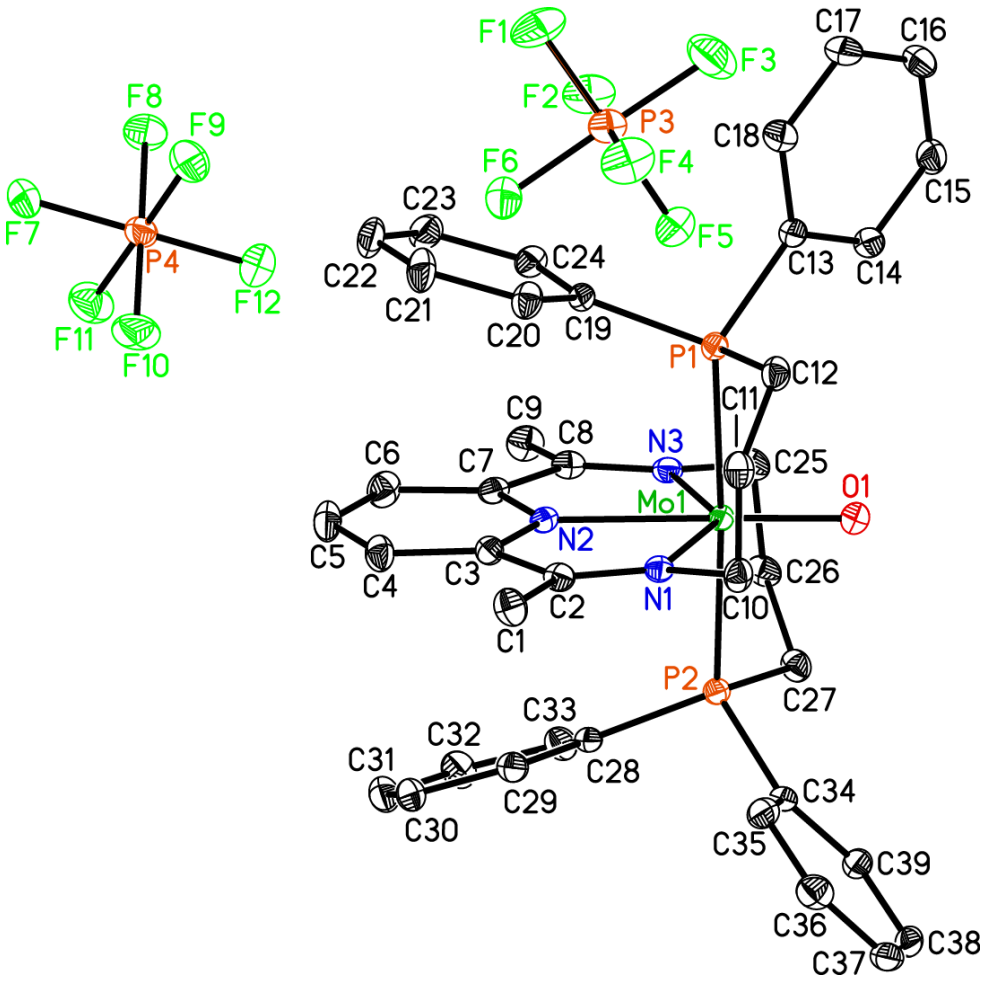

Figure S1. The molecular structure of **2** shown at 30% probability ellipsoids. Hydrogen atoms and co-crystallized acetone molecules are omitted for clarity.

Table S2. Bond distances (Å) and angles (°) determined for **2**.

Mo1-O1	1.693(2)	C5-C6	1.386(5)	C29-C30	1.385(4)
Mo1-N3	2.134(2)	C6-C7	1.393(4)	C30-C31	1.381(5)
Mo1-N1	2.140(2)	C7-C8	1.480(4)	C31-C32	1.379(5)
Mo1-N2	2.240(2)	C8-C9	1.486(4)	C32-C33	1.389(4)
Mo1-P1	2.5264(8)	C10-C11	1.529(4)	C34-C35	1.390(4)
Mo1-P2	2.5371(8)	C11-C12	1.537(4)	C34-C39	1.392(4)
P1-C19	1.808(3)	C13-C14	1.390(4)	C35-C36	1.384(4)
P1-C13	1.825(3)	C13-C18	1.398(4)	C36-C37	1.379(5)
P1-C12	1.838(3)	C14-C15	1.383(4)	C37-C38	1.373(5)
P2-C28	1.821(3)	C15-C16	1.383(5)	C38-C39	1.382(4)
P2-C34	1.821(3)	C16-C17	1.374(5)	P3-F3	1.585(2)
P2-C27	1.840(3)	C17-C18	1.387(5)	P3-F2	1.591(2)
N1-C2	1.294(4)	C19-C20	1.384(4)	P3-F1	1.595(2)
N1-C10	1.487(4)	C19-C24	1.395(4)	P3-F6	1.597(2)
N2-C7	1.339(4)	C20-C21	1.391(4)	P3-F4	1.602(2)
N2-C3	1.348(4)	C21-C22	1.386(5)	P3-F5	1.604(2)
N3-C8	1.301(4)	C22-C23	1.380(5)	P4-F10	1.595(2)
N3-C25	1.481(4)	C23-C24	1.380(4)	P4-F8	1.598(2)
C1-C2	1.498(4)	C25-C26	1.539(4)	P4-F9	1.599(2)
C2-C3	1.469(4)	C26-C27	1.540(4)	P4-F11	1.599(2)
C3-C4	1.388(4)	C28-C33	1.388(4)	P4-F12	1.599(2)
C4-C5	1.387(5)	C28-C29	1.395(4)	P4-F7	1.603(2)

O1-Mo1-N3	109.98(10)	C34-P2-Mo1	113.02(10)	C7-C8-C9	118.5(3)
O1-Mo1-N1	110.08(10)	C27-P2-Mo1	104.45(10)	N1-C10-C11	109.1(2)
N3-Mo1-N1	139.92(9)	C2-N1-C10	120.4(2)	C10-C11-C12	115.2(3)
O1-Mo1-N2	179.10(9)	C2-N1-Mo1	123.9(2)	C11-C12-P1	119.3(2)
N3-Mo1-N2	69.88(9)	C10-N1-Mo1	114.68(18)	C14-C13-C18	119.5(3)
N1-Mo1-N2	70.05(9)	C7-N2-C3	120.7(2)	C14-C13-P1	121.4(2)
O1-Mo1-P1	91.23(7)	C7-N2-Mo1	119.95(19)	C18-C13-P1	119.0(2)
N3-Mo1-P1	102.23(7)	C3-N2-Mo1	119.35(19)	C15-C14-C13	120.0(3)
N1-Mo1-P1	78.11(6)	C8-N3-C25	120.8(3)	C16-C15-C14	120.2(3)
N2-Mo1-P1	89.67(6)	C8-N3-Mo1	124.3(2)	C17-C16-C15	120.2(3)
O1-Mo1-P2	91.85(7)	C25-N3-Mo1	113.71(18)	C16-C17-C18	120.4(3)
N3-Mo1-P2	77.35(7)	N1-C2-C3	114.5(3)	C17-C18-C13	119.7(3)
N1-Mo1-P2	100.15(6)	N1-C2-C1	126.6(3)	C20-C19-C24	119.9(3)
N2-Mo1-P2	87.25(6)	C3-C2-C1	118.8(3)	C20-C19-P1	124.0(2)
P1-Mo1-P2	176.84(2)	N2-C3-C4	121.1(3)	C24-C19-P1	116.0(2)
C19-P1-C13	105.72(14)	N2-C3-C2	112.1(2)	C19-C20-C21	119.3(3)
C19-P1-C12	110.36(14)	C4-C3-C2	126.7(3)	C22-C21-C20	120.4(3)
C13-P1-C12	100.64(14)	C5-C4-C3	118.1(3)	C23-C22-C21	120.4(3)
C19-P1-Mo1	112.75(9)	C6-C5-C4	120.7(3)	C24-C23-C22	119.4(3)
C13-P1-Mo1	120.13(10)	C5-C6-C7	118.1(3)	C23-C24-C19	120.6(3)
C12-P1-Mo1	106.44(10)	N2-C7-C6	121.2(3)	N3-C25-C26	110.2(2)
C28-P2-C34	108.07(13)	N2-C7-C8	111.9(3)	C25-C26-C27	115.7(2)
C28-P2-C27	106.98(14)	C6-C7-C8	126.9(3)	C26-C27-P2	117.6(2)
C34-P2-C27	105.80(14)	N3-C8-C7	113.9(3)	C33-C28-C29	118.4(3)
C28-P2-Mo1	117.66(9)	N3-C8-C9	127.5(3)	C33-C28-P2	122.2(2)

C29-C28-P2	119.2(2)	F3-P3-F1	90.96(14)	F10-P4-F9	90.44(12)
C30-C29-C28	120.9(3)	F2-P3-F1	89.94(12)	F8-P4-F9	90.05(12)
C31-C30-C29	119.5(3)	F3-P3-F6	179.04(15)	F10-P4-F11	89.38(12)
C32-C31-C30	120.6(3)	F2-P3-F6	89.79(12)	F8-P4-F11	90.13(12)
C31-C32-C33	119.6(3)	F1-P3-F6	89.93(13)	F9-P4-F11	179.23(13)
C28-C33-C32	120.8(3)	F3-P3-F4	89.42(14)	F10-P4-F12	90.26(13)
C35-C34-C39	119.0(3)	F2-P3-F4	178.75(13)	F8-P4-F12	89.98(12)
C35-C34-P2	118.6(2)	F1-P3-F4	91.31(13)	F9-P4-F12	90.43(12)
C39-C34-P2	122.3(2)	F6-P3-F4	90.21(13)	F11-P4-F12	90.32(13)
C36-C35-C34	120.2(3)	F3-P3-F5	90.15(13)	F10-P4-F7	90.01(12)
C37-C36-C35	120.2(3)	F2-P3-F5	89.89(12)	F8-P4-F7	89.75(11)
C38-C37-C36	119.9(3)	F1-P3-F5	178.88(13)	F9-P4-F7	89.96(12)
C37-C38-C39	120.5(3)	F6-P3-F5	88.96(12)	F11-P4-F7	89.29(12)
C38-C39-C34	120.1(3)	F4-P3-F5	88.86(12)	F12-P4-F7	179.53(14)
F3-P3-F2	90.56(13)	F10-P4-F8	179.45(14)		

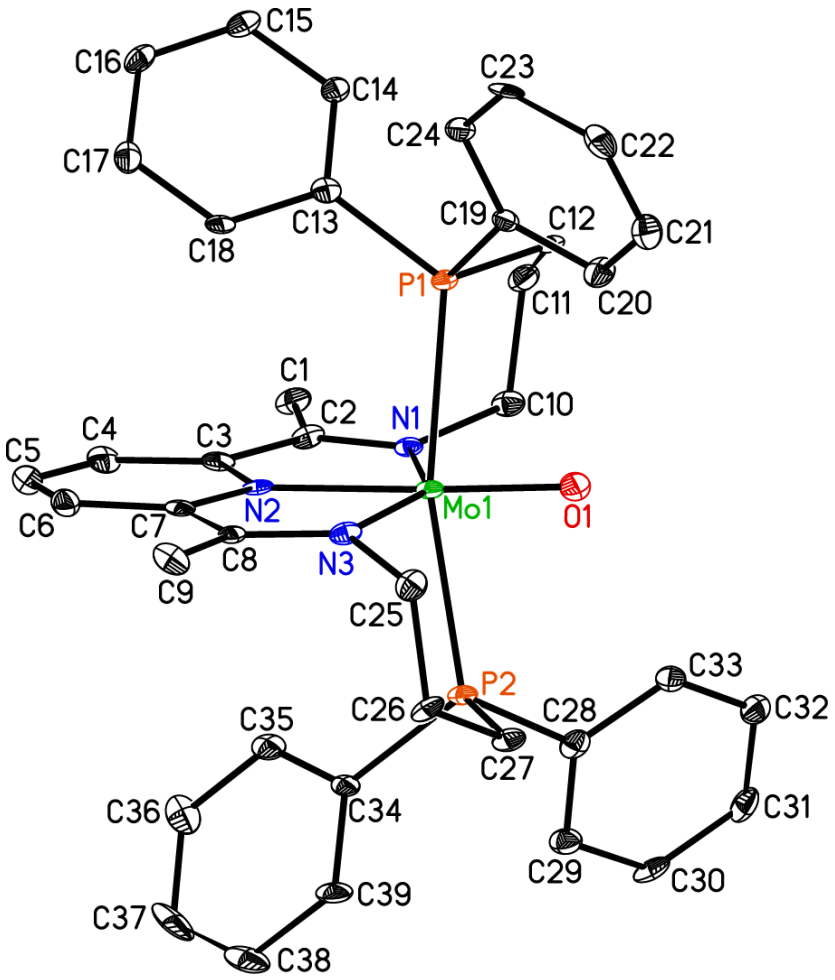

Figure S2. The molecular structure of **3** displayed with 30% probability ellipsoids. Hydrogen atoms omitted for clarity.

Table S3. Bond distances (Å) and angles (°) determined for **3**.

Mo1-O1	1.797(3)	C1-C2	1.492(7)	C20-C21	1.373(7)
Mo1-N1	2.062(4)	C2-C3	1.420(7)	C21-C22	1.392(7)
Mo1-N3	2.068(4)	C3-C4	1.396(6)	C22-C23	1.386(7)
Mo1-N2	2.101(3)	C4-C5	1.384(7)	C23-C24	1.374(7)
Mo1-P2	2.5085(14)	C5-C6	1.396(7)	C25-C26	1.514(6)
Mo1-P1	2.5301(14)	C6-C7	1.399(6)	C26-C27	1.534(7)
P1-C13	1.820(5)	C7-C8	1.401(7)	C28-C33	1.395(6)
P1-C19	1.828(5)	C8-C9	1.498(7)	C28-C29	1.400(7)
P1-C12	1.831(5)	C10-C11	1.533(6)	C29-C30	1.394(7)
P2-C34	1.826(5)	C11-C12	1.540(7)	C30-C31	1.362(7)
P2-C27	1.836(5)	C13-C18	1.399(6)	C31-C32	1.393(7)
P2-C28	1.837(5)	C13-C14	1.402(7)	C32-C33	1.379(7)
N1-C2	1.355(5)	C14-C15	1.379(6)	C34-C35	1.384(7)
N1-C10	1.480(6)	C15-C16	1.379(7)	C34-C39	1.393(7)
N2-C7	1.398(6)	C16-C17	1.378(7)	C35-C36	1.382(6)
N2-C3	1.410(6)	C17-C18	1.395(6)	C36-C37	1.395(8)
N3-C8	1.363(5)	C19-C24	1.393(7)	C37-C38	1.369(8)
N3-C25	1.474(6)	C19-C20	1.397(6)	C38-C39	1.382(7)

O1-Mo1-N1	110.29(15)	C7-N2-C3	118.9(4)	C16-C17-C18	120.5(5)
O1-Mo1-N3	105.81(16)	C7-N2-Mo1	120.4(3)	C17-C18-C13	119.4(5)
N1-Mo1-N3	143.90(14)	C3-N2-Mo1	120.6(3)	C24-C19-C20	118.2(5)
O1-Mo1-N2	176.61(16)	C8-N3-C25	118.7(4)	C24-C19-P1	123.6(4)
N1-Mo1-N2	71.98(15)	C8-N3-Mo1	122.9(3)	C20-C19-P1	118.1(4)
N3-Mo1-N2	71.93(15)	C25-N3-Mo1	117.4(3)	C21-C20-C19	120.3(5)
O1-Mo1-P2	83.50(11)	N1-C2-C3	112.4(4)	C20-C21-C22	121.1(5)
N1-Mo1-P2	100.44(11)	N1-C2-C1	123.5(4)	C23-C22-C21	118.8(5)
N3-Mo1-P2	84.11(11)	C3-C2-C1	124.2(4)	C24-C23-C22	120.3(5)
N2-Mo1-P2	98.66(11)	C4-C3-N2	120.7(5)	C23-C24-C19	121.3(5)
O1-Mo1-P1	83.65(11)	C4-C3-C2	128.1(5)	N3-C25-C26	111.9(4)
N1-Mo1-P1	81.27(11)	N2-C3-C2	111.2(4)	C25-C26-C27	115.3(4)
N3-Mo1-P1	102.31(11)	C5-C4-C3	120.1(5)	C26-C27-P2	113.9(3)
N2-Mo1-P1	94.31(11)	C4-C5-C6	119.8(5)	C33-C28-C29	119.1(5)
P2-Mo1-P1	166.80(4)	C5-C6-C7	120.7(5)	C33-C28-P2	118.2(4)
C13-P1-C19	104.2(2)	N2-C7-C6	119.8(5)	C29-C28-P2	122.6(4)
C13-P1-C12	105.2(2)	N2-C7-C8	112.1(4)	C30-C29-C28	119.5(5)
C19-P1-C12	101.5(2)	C6-C7-C8	128.1(5)	C31-C30-C29	120.9(5)
C13-P1-Mo1	121.00(16)	N3-C8-C7	112.5(4)	C30-C31-C32	120.1(5)
C19-P1-Mo1	119.47(18)	N3-C8-C9	122.9(5)	C33-C32-C31	120.0(5)
C12-P1-Mo1	102.85(17)	C7-C8-C9	124.6(4)	C32-C33-C28	120.4(5)
C34-P2-C27	106.0(2)	N1-C10-C11	112.2(4)	C35-C34-C39	119.6(5)
C34-P2-C28	103.1(2)	C10-C11-C12	114.4(5)	C35-C34-P2	118.1(4)
C27-P2-C28	103.4(2)	C11-C12-P1	116.1(3)	C39-C34-P2	122.2(4)
C34-P2-Mo1	118.94(16)	C18-C13-C14	118.6(4)	C36-C35-C34	120.7(5)
C27-P2-Mo1	104.96(17)	C18-C13-P1	118.0(4)	C35-C36-C37	119.0(6)
C28-P2-Mo1	118.80(17)	C14-C13-P1	123.3(3)	C38-C37-C36	120.5(5)
C2-N1-C10	118.3(4)	C15-C14-C13	121.5(5)	C37-C38-C39	120.4(6)
C2-N1-Mo1	123.8(3)	C14-C15-C16	119.1(5)	C38-C39-C34	119.7(6)
C10-N1-Mo1	116.6(3)	C17-C16-C15	120.8(5)		

SPECTROSCOPIC DATA

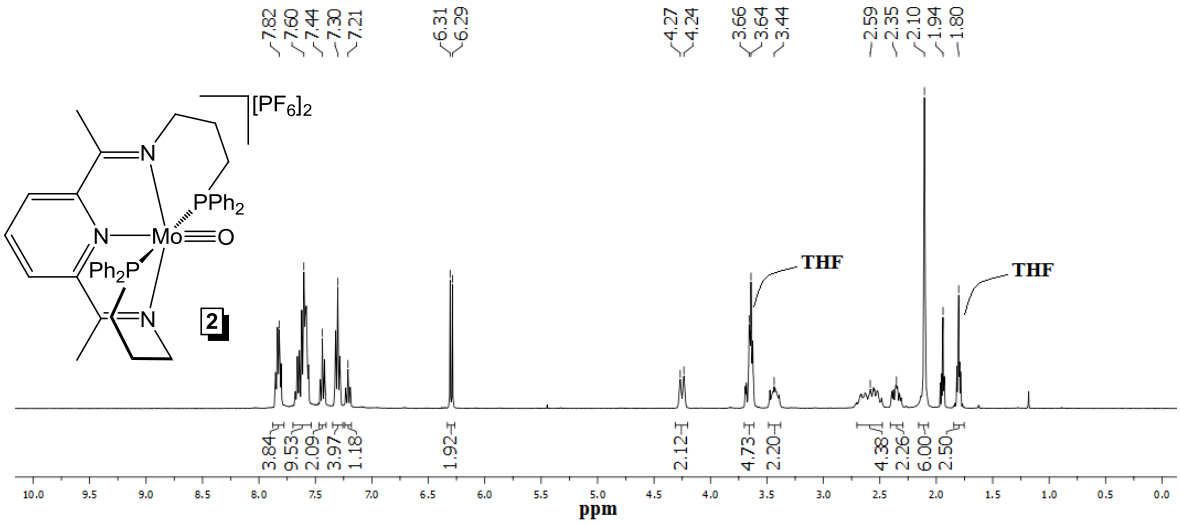

Figure S3. ^{1}H NMR spectrum of **2** in acetonitrile-d_3.

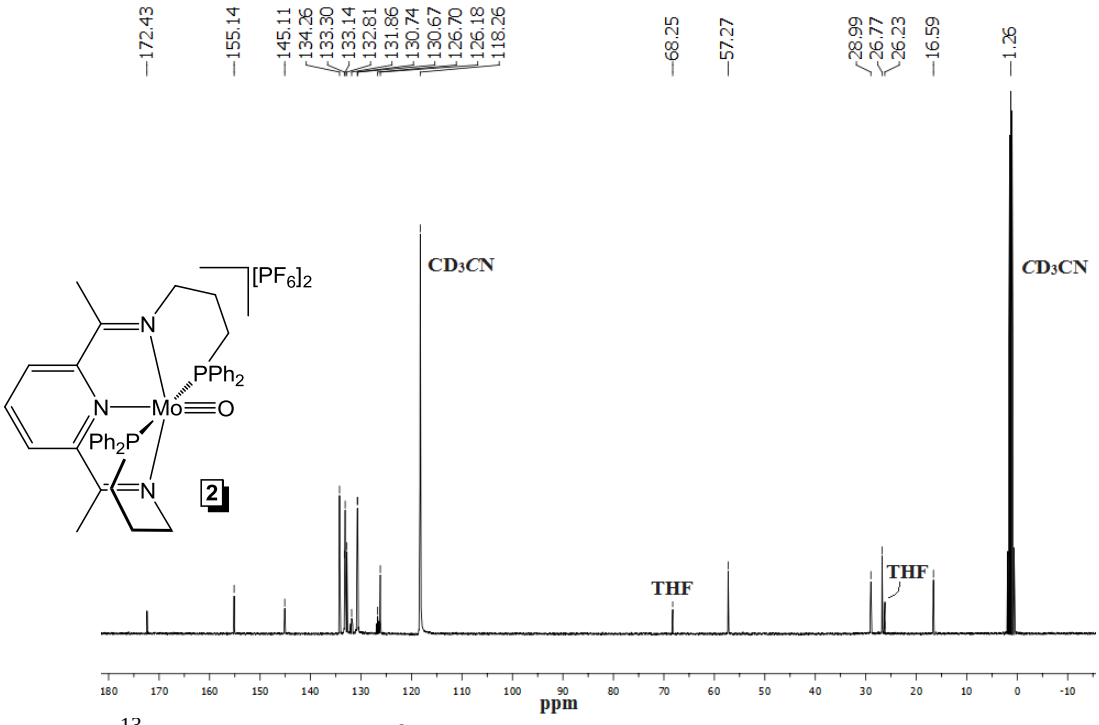

Figure S4. ^{13}C NMR spectrum of **2** in acetonitrile-d_3.

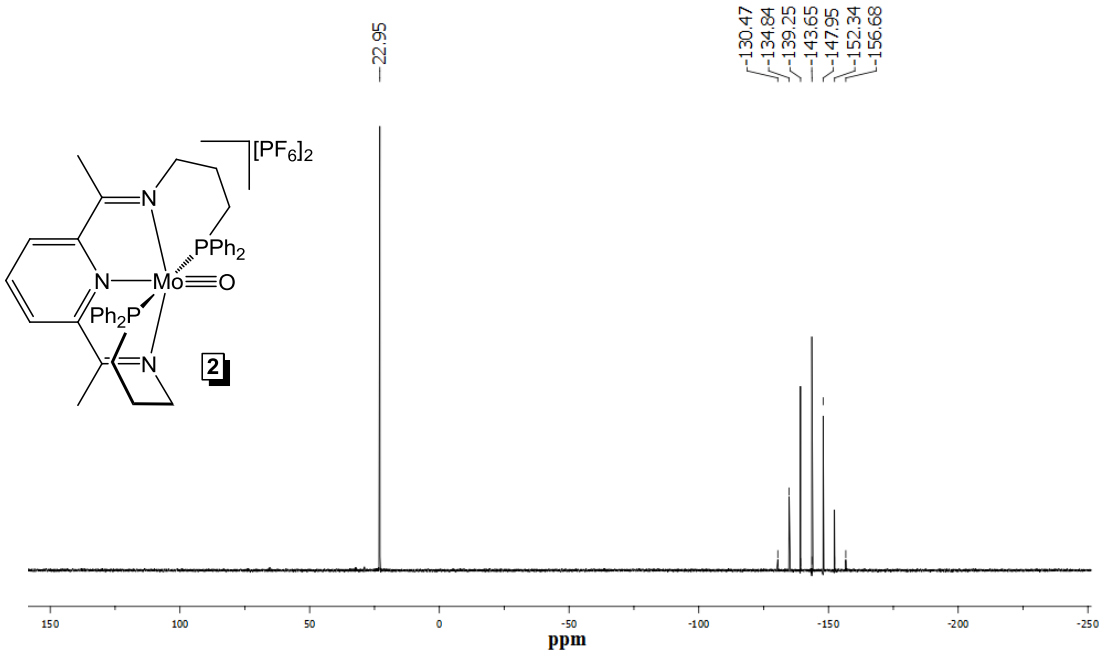

Figure S5. ^{31}P NMR spectrum of **2** in acetonitrile-d_3.

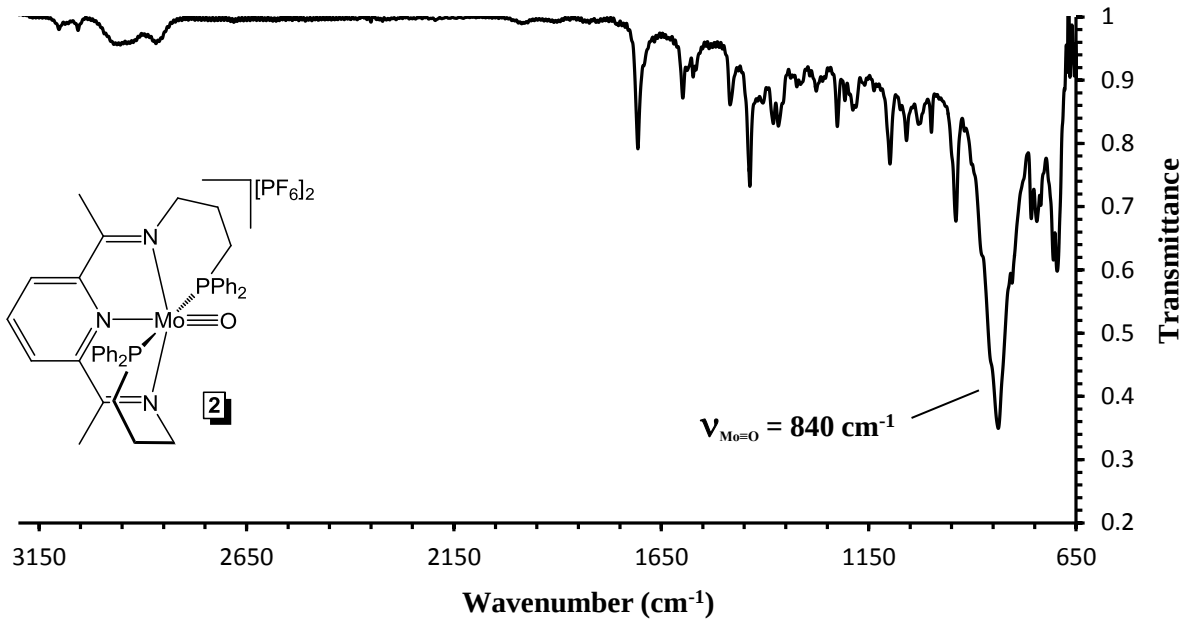

Figure S6. IR spectrum of **2** in KBr.

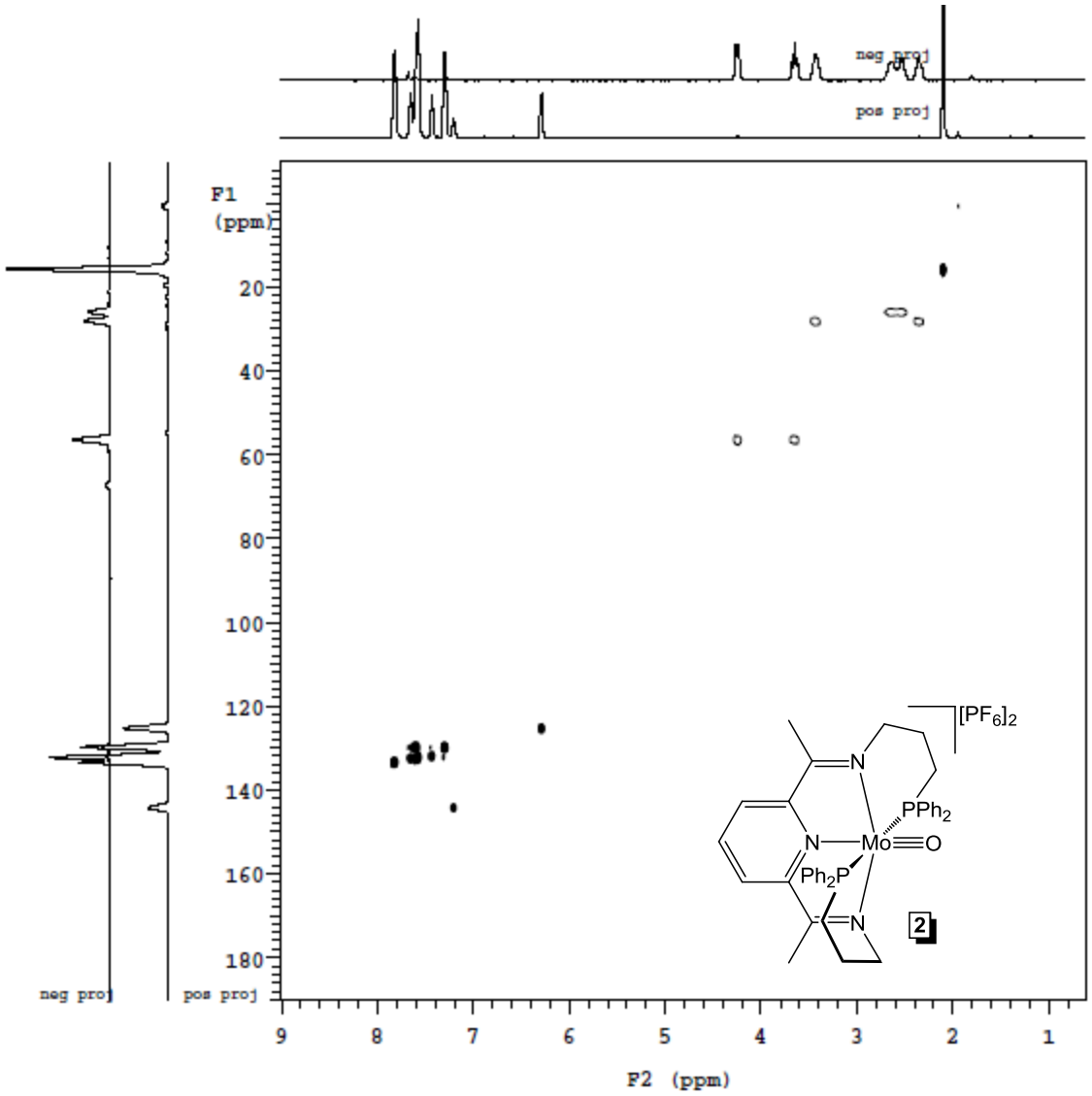

Figure S7. gHSQCAD NMR spectrum of **2** in acetonitrile-d_3.

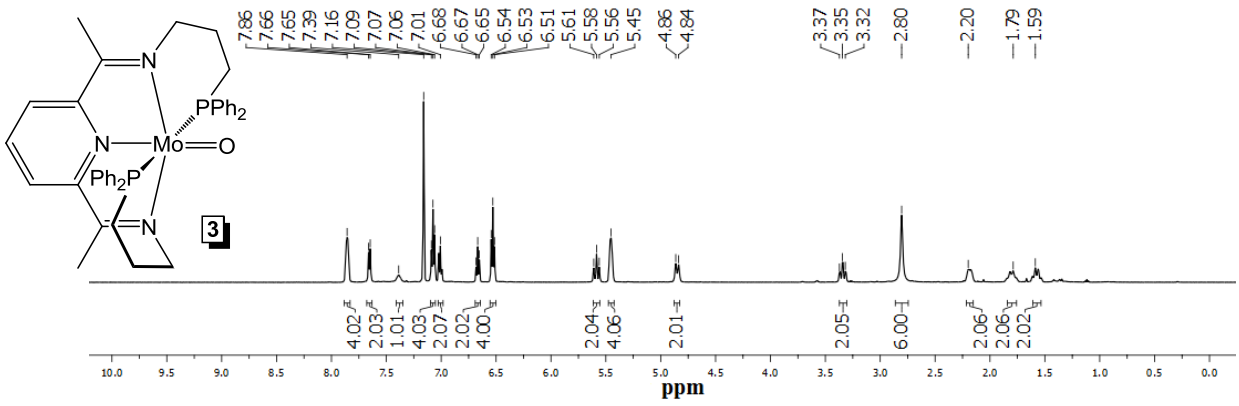

Figure S8. ^{1}H NMR spectrum of **3** in benzene-d_6.

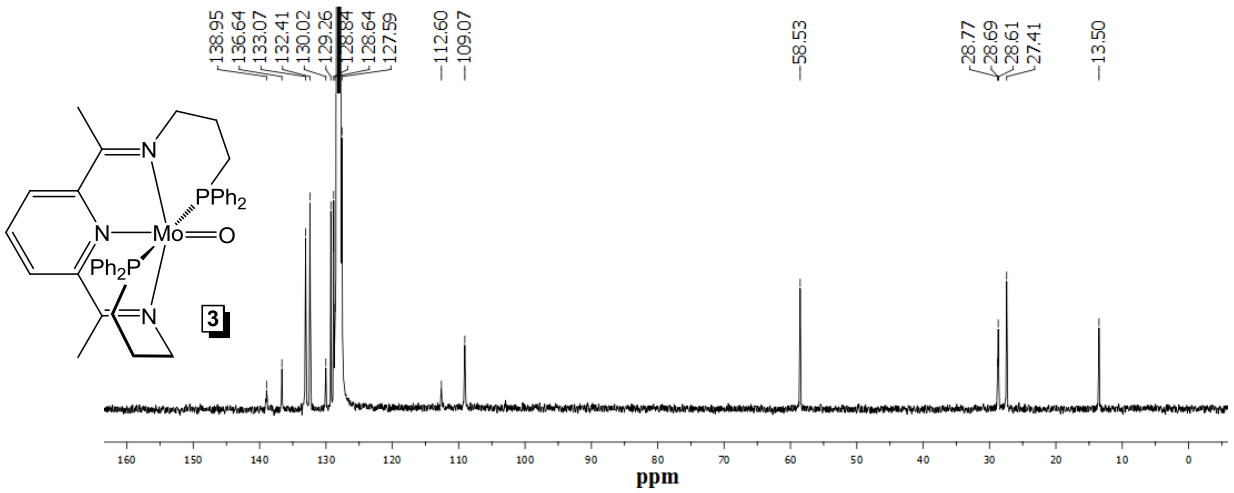

Figure S9. ^{13}C NMR spectrum of **3** in benzene-d_6.

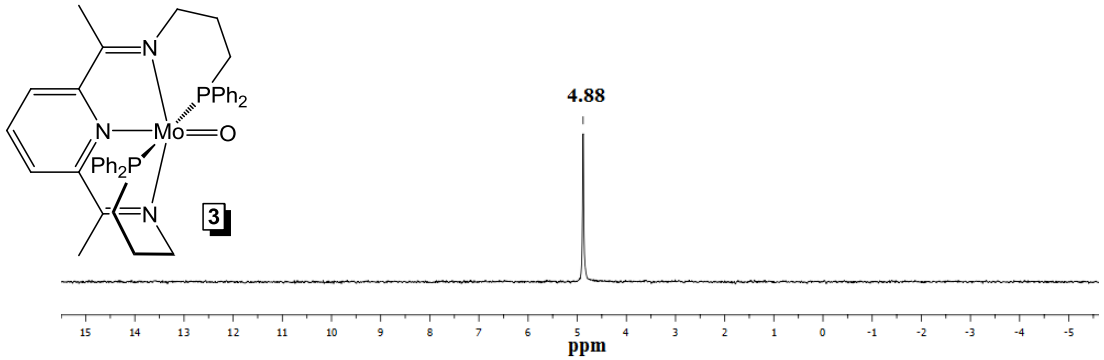

Figure S10. ^{31}P NMR spectrum of **3** in benzene-d_6.

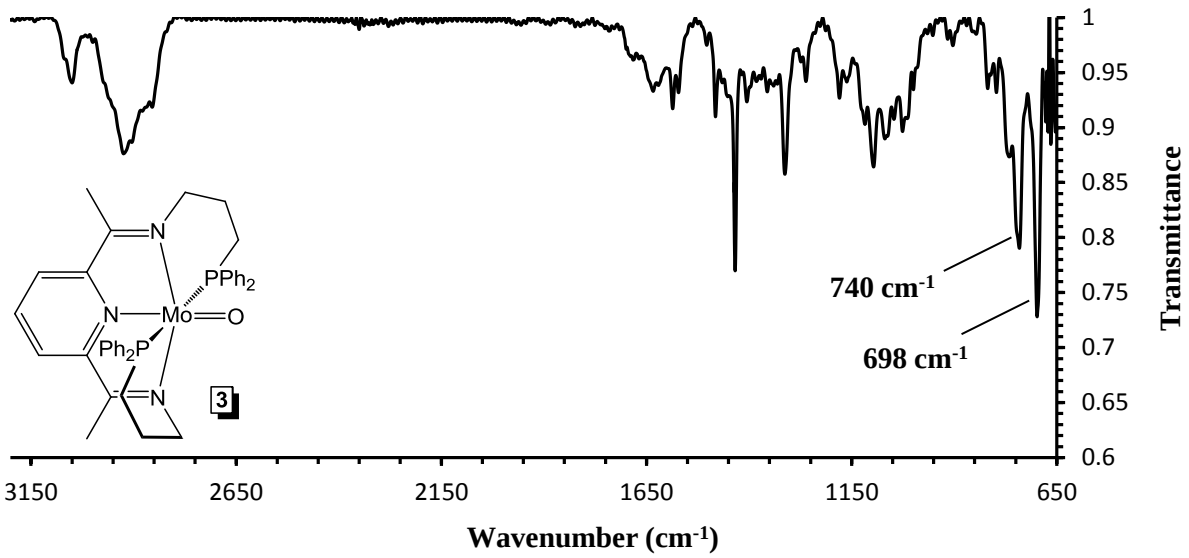

Figure S11. IR spectrum of **3** in KBr.

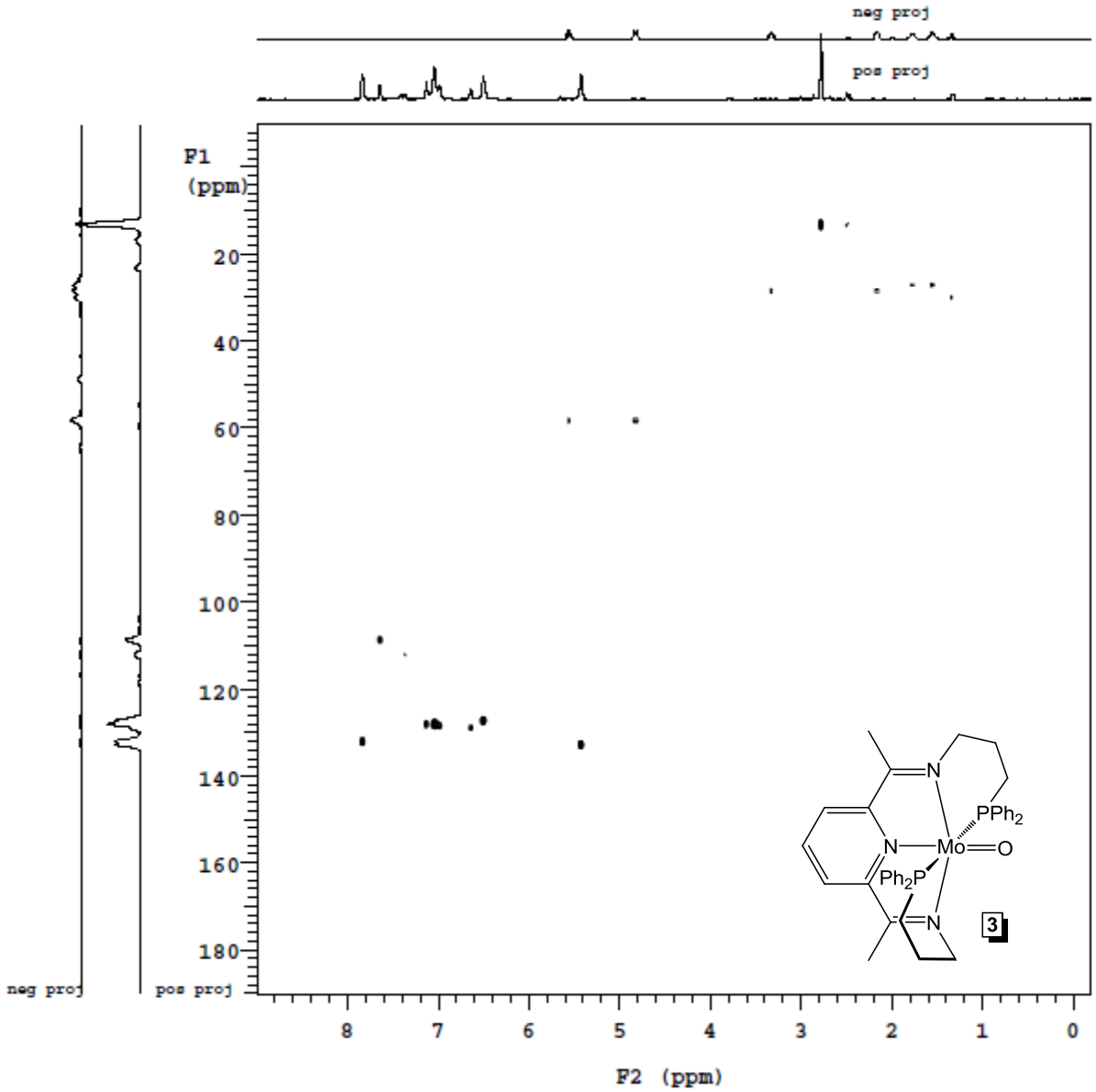

Figure S12. gHSQCAD NMR spectrum of **3** in benzene-d_6.

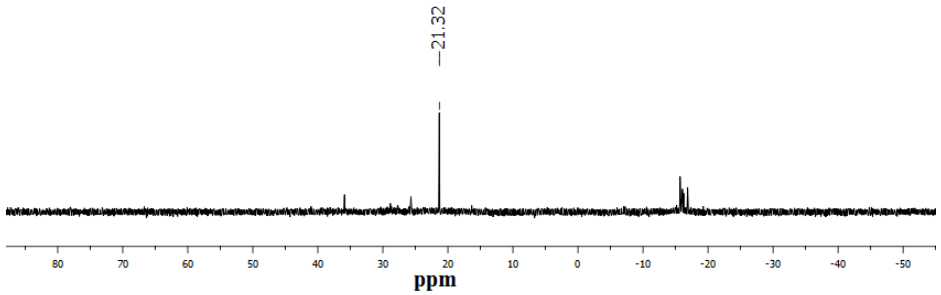

Figure S13. ^{31}P NMR spectrum collected after adding 4 atm of H_2 to **3** in benzene-d_6. The new resonance at 21.32 ppm is consistent with formation of a C_2-symmetric complex, presumed to be **5**. Unidentified side products are also observed.

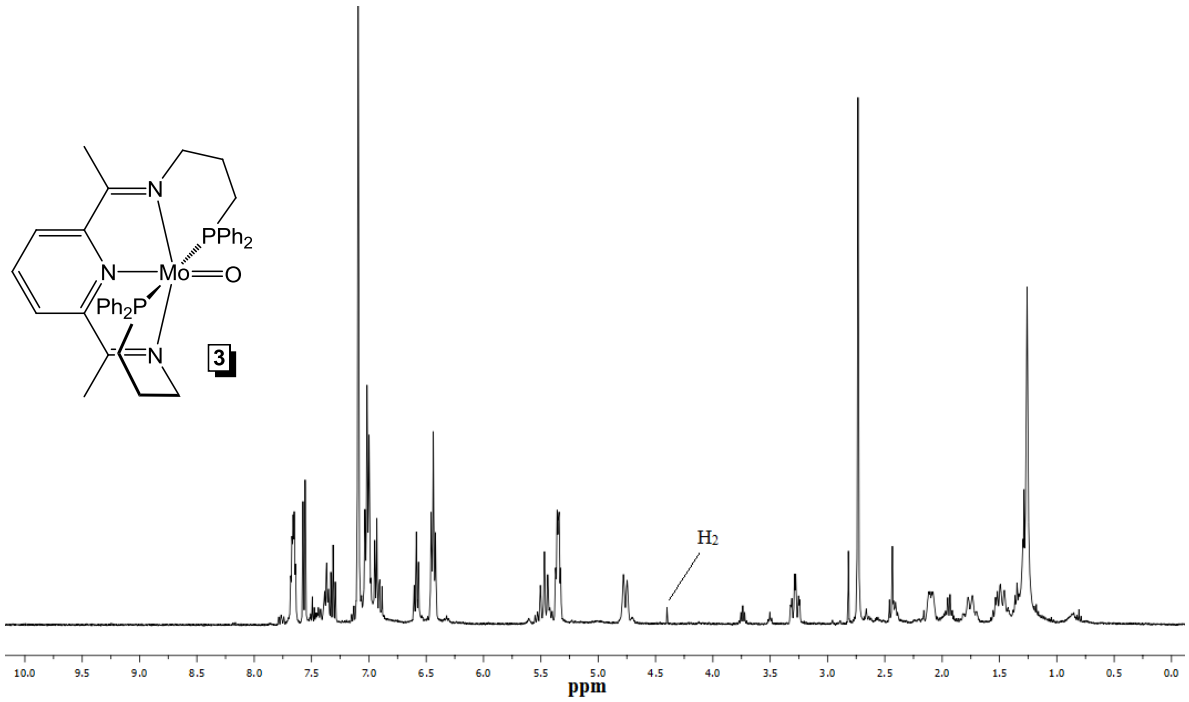

Figure S14. ^{1}H NMR spectrum of **3** in benzene-d_6 obtained from stoichiometric H_2O addition to (κ^6-*P*,*N*,*N*,*N*,*C*,*P*-^{Ph2PPr}PDI)MoH.

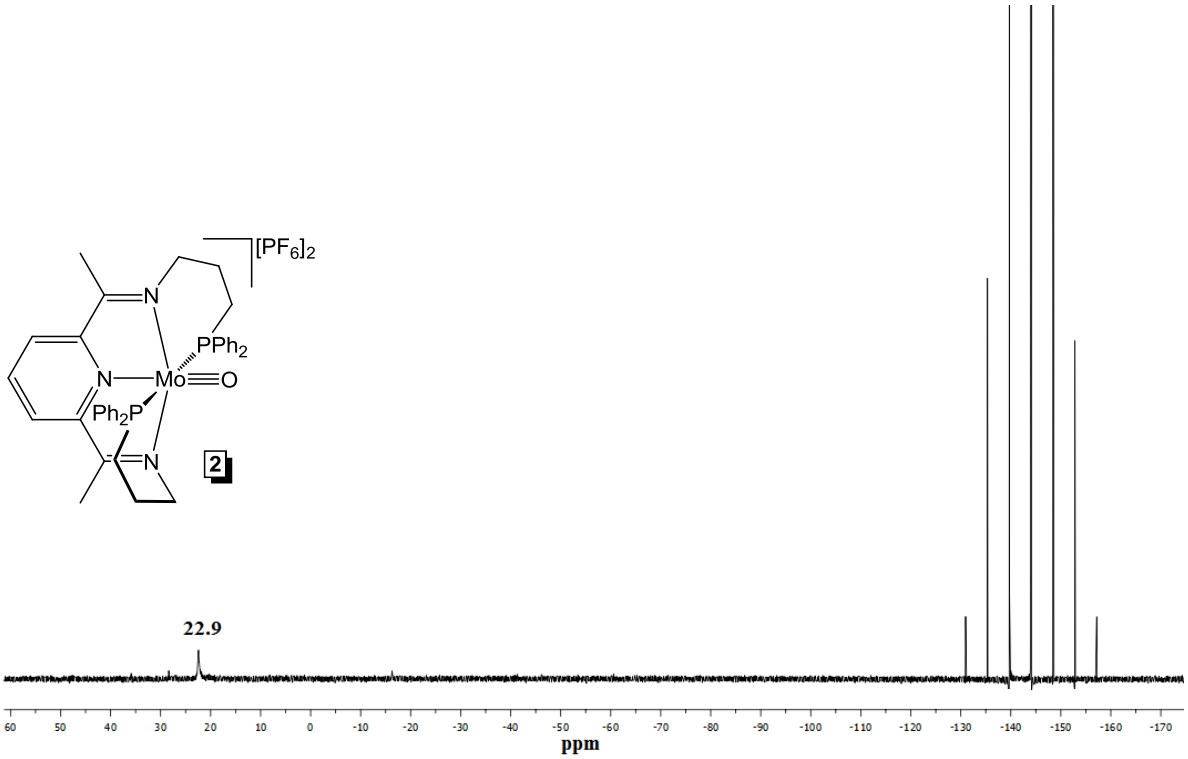

Figure S15. ^{31}P NMR spectrum of **2** in acetonitrile after bulk electrolysis with D_2O.

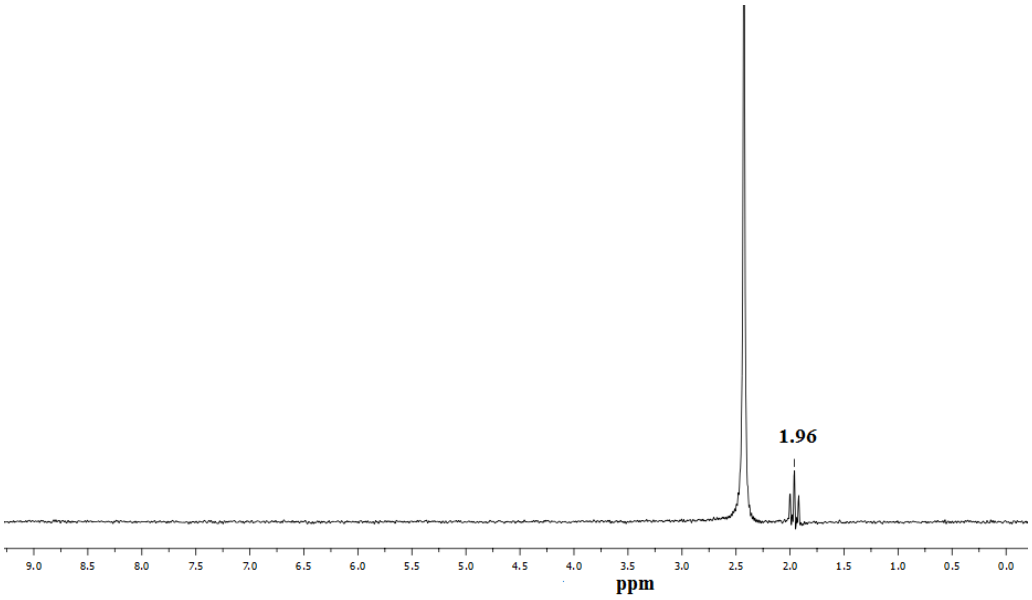

Figure S16. ^{2}H NMR spectrum of **2** in acetonitrile after bulk electrolysis with D_2O. The peak at 1.96 ppm is due to $NCCH_2D$.

ELECTROCHEMICAL DATA

Table S4. Overpotential calculated from the open circuit potential (OCP) vs $Fc^{+/0}$ and $E_{p/2}$ of the catalytic wave associated with **2** at the specified concentration of water in acetonitrile.

[H_2O] (M)	**OCP (V vs $Fc^{+/0}$)**	**$E_{p/2}$ (V vs $Fc^{+/0}$)**	**Overpotential, OCP - $E_{p/2}$ (V)**
0.2	-1.10	-2.75	1.65
0.4	-1.07	-2.74	1.67
0.6	-1.12	-2.70	1.58
1.8	-1.08	-2.68	1.60
2.0	-1.08	-2.69	1.61
3.5	-1.03	-2.65	1.62
4.0	-1.03	-2.65	1.62
5.0	-1.01	-2.64	1.63
6.0	-0.94	-2.64	1.70

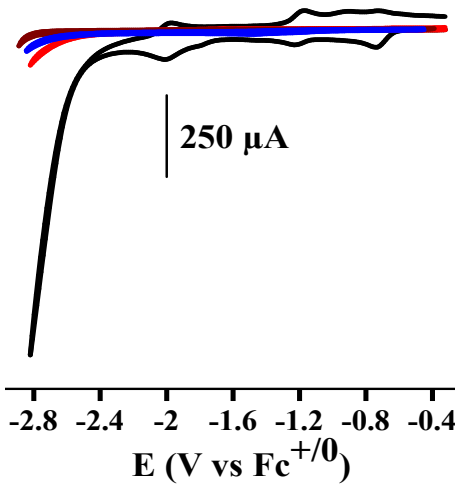

Figure S17. Cyclic voltammogram from 2.0 mM **2** in 3.5 M water in acetonitrile containing 0.1 M $TBAPF_6$ (black). Control experiments employing a rinsed working electrode immediately following electrocatalysis and transferred to a neat acetonitrile solution containing 0 M (dark red) and 5.0 M water (red). To illustrate that catalysis at a glassy carbon electrode is negligible, a solution of acetonitrile containing 6.0 M water in the absence of catalyst is shown (blue). Potential scan rate is 0.2 V s^{-1}.

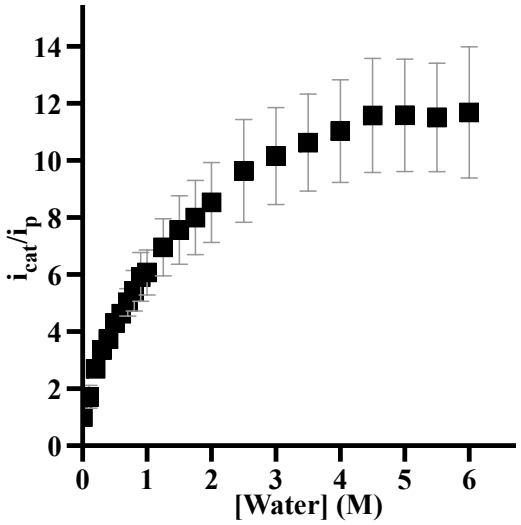

Figure S18. Dependence of normalized catalytic current (i_{cat}/i_p) on the concentration of water present. Data (squares, $k = 55 \pm 15$ s^{-1}) are averaged from three individual experiments and error bars represent one standard deviation. Experimental conditions: acetonitrile containing 0.1 M $TBAPF_6$ and a scan rate of 0.2 V s^{-1}.

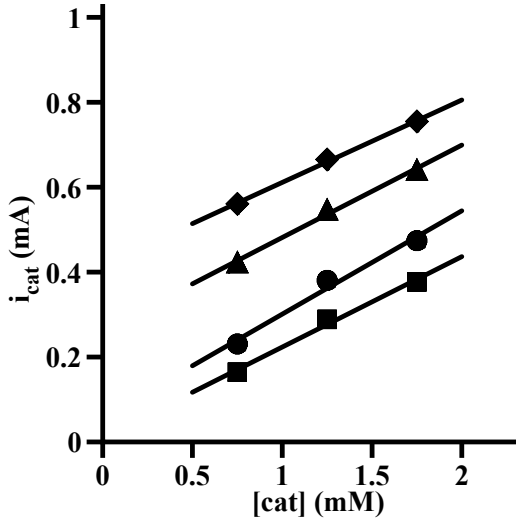

Figure S19. Catalytic current depends linearly on the concentration of **2** present in the experiment irrespective of water concentrations. Squares, circles, triangles, and diamonds refer to 0.3, 0.6, 1.75, and 3.0 M water, respectively. Solid lines are the lines of best fit with $R^2 = 0.99$.

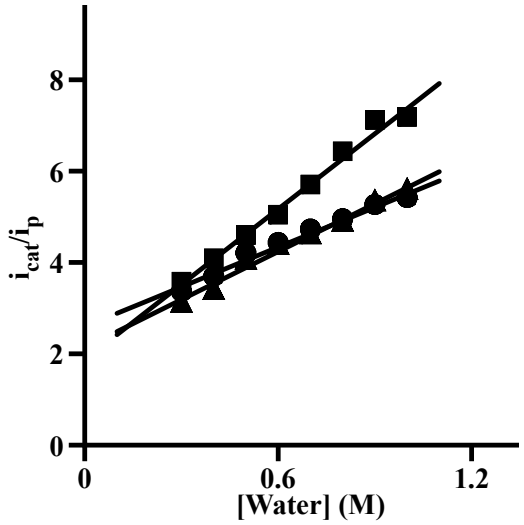

Figure S20. Dependence of normalized catalytic current on water concentration. Triangles, squares, and circles refer to currents extracted from cyclic voltammograms at -2.8 V vs $Fc^{+/0}$ for solutions containing **2** at 0.75, 1.25, and 1.75 mM, respectively. Solid lines are the lines of best fit ($R^2 = 0.98$). Experimental conditions: acetonitrile containing 0.1 M $TBAPF_6$ with a scan rate of 0.2 V s^{-1}. Averaging the rate constant obtained from these three individual experiments (in the water concentration range of 0.3 to 1.0 M) yields $k = 25 \pm 5$ s^{-1}.

DISFAVORED MECHANISTIC PATHWAY

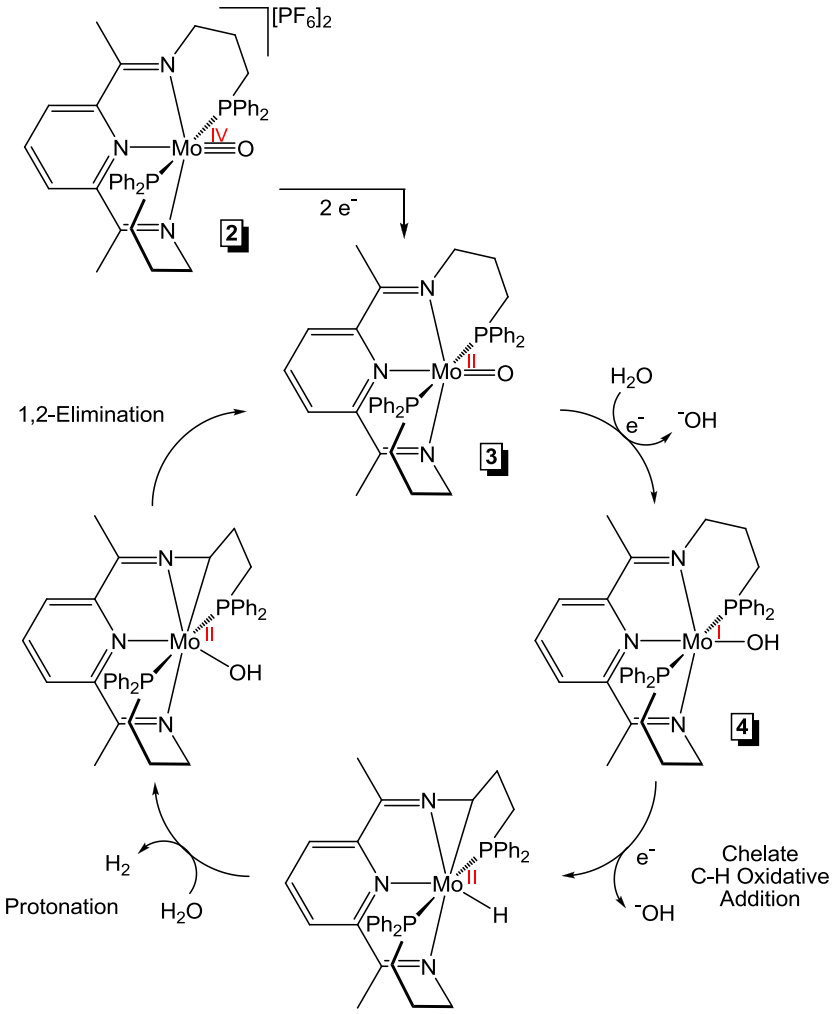

Figure S21. Disfavored ligand-assisted electrocatalytic cycle for generation of H_2 and hydroxide ions from water.

REFERENCES

[1] Li, Y.; Li, Z.; Li, F.; Wang, Q.; Tao, F. *Tetrahedron Lett.* **2005**, *46*, 6159-6162.

[2] Ben-Daat, H.; Hall, G. B.; Groy, T. L.; Trovitch, R. J. *Eur. J. Inorg. Chem.* **2013**, 4430-4442.

[3] Pal, R.; Groy, T. L.; Trovitch, R. J. *Inorg. Chem.* **2015**, *54*, 7506-7515.

[4] Roberts, J. A. S.; Bullock, R. M. *Inorg. Chem.* **2013**, *52*, 3823-3835.